HHS Public Access

Author manuscript

Virology. Author manuscript; available in PMC 2018 February 14.

Published in final edited form as:

Virology. 2012 November 10; 433(1): 35–44. doi:10.1016/j.virol.2012.07.011.

Mutations in the West Nile prM protein affect VLP and virion secretion *in vitro*

Amanda E. Calvert[a,*], **Claire Y.-H. Huang**[a], **Carol D. Blair**[b], and **John T. Roehrig**[a]

[a]Arbovirus Diseases Branch, Division of Vector-Borne Diseases, Centers for Disease Control and Prevention, Public Health Service, U.S. Department of Health and Human Services, 3150 Rampart Rd., Fort Collins, CO 80521, USA

[b]Department of Microbiology, Immunology and Pathology, Colorado State University, Fort Collins, CO 80523, USA

Abstract

Mutation of the West Nile virus-like particle (WN VLP) prM protein (T20D, K31A, K31V, or K31T) results in undetectable VLP secretion from transformed COS-1 cells. K31 mutants formed intracellular prM-E heterodimers; however these proteins remained in the ER and ER–Golgi intermediary compartments of transfected cells. The T20D mutation affected glycosylation, heterodimer formation, and WN VLP secretion. When infectious viruses bearing the same mutations were used to infect COS-1 cells, K31 mutant viruses exhibited delayed growth and reduced infectivity compared to WT virus. Epitope maps of WN VLP and WNV prM were also different. These results suggest that while mutations in the prM protein can reduce or eliminate secretion of WN VLPs, they have less effect on virus. This difference may be due to the quantity of prM in WN VLPs compared to WNV or to differences in maturation, structure, and symmetry of these particles.

Keywords

Flavivirus; West Nile virus; prM protein; Flavivirus structure

Introduction

West Nile virus (WNV) is an emerging global pathogen causing WN fever and meningoencephalitis. Since its introduction into the Western Hemisphere in 1999 it has spread throughout North and Central America and the Caribbean and currently is the leading cause of mosquito-borne human encephalitis in the region (Mackenzie et al., 2004). WNV is a member of the family *Flaviviridae*, genus *Flavivirus*. It is maintained in an enzootic cycle between mosquitoes and birds with humans and other mammals as incidental hosts (Mackenzie et al., 2004). Other medically important flaviviruses include Japanese encephalitis virus (JEV), tick-borne encephalitis virus (TBEV), yellow fever virus, and the four serotypes of dengue viruses (DENV).

*Corresponding author. Fax: +1 970 494 6631. zpz0@cdc.gov (A.E. Calvert).

WNV has a single-stranded, positive sense 11 kb RNA genome that encodes 3 structural proteins at its 5′-end. The envelope (E) protein is the major virion glycoprotein responsible for virus membrane attachment and fusion. The capsid (C) protein binds the genomic RNA to form the nucleocapsid. The pre-membrane (prM) protein is a chaperone that assists in the maturation of the E protein, and occurs as a prM-E heterodimer. The prM-E heterodimers form 60 trimeric spikes on the surface of the immature DEN2 virion that measures 600 Å in diameter (Li et al., 2008). The pr peptide is the amino terminal part of the prM protein that is cleaved from prM during virion maturation by the host multibasic-recognition protease furin. The pr remains associated with the virion to protect the fusion loop of the E protein from premature fusion until reaching an extracellular neutral pH environment. Once the virion reaches a neutral pH, the pr peptide dissociates, resulting in the formation of a fusion-competent particle (Yu et al., 2009). Since this cleavage by furin can be inefficient, and appears to be host-cell dependent, not all virions released from cells contain mature M and in fact, there is likely populations of virions containing M, prM or a mixture of prM and M on the virion surface as demonstrated by cryo-electron microscopy (Cherrier et al., 2009; Junjhon et al., 2010; Pokidysheva et al., 2006; Zhang et al., 2003). The existence of prM in infectious flavivirus particles has also been established with experiments measuring pH sensitivity, viral tropism and neutralization capacity of antibodies with less accessible sites on E when prM is present (Davis et al., 2006; Guirakhoo et al., 1992; Nelson et al., 2008).

The polyprotein encoded by the flavivirus RNA genome is translated in association with the rough endoplasmic reticulum (ER). Several transmembrane domains of the polyprotein traverse the ER membrane and co- and post-translational cleavages to produce functional products are carried out by the host enzyme signalase and the virally-encoded protease NS2B-3 (Lindenbach and Rice, 2003). The viral structural proteins prM and E form dimers on the ER membrane, producing an icosahedral scaffold that may or may not enclose the viral RNA genome packaged in the nucleocapsid (Konishi et al., 1992; Schalich et al., 1996). The virus particles acquire their lipid bilayer envelopes as they bud into the lumen of the ER and are transported through the Golgi for further envelope protein modification, including glycosylation of the structural proteins and cleavage of the pr peptide from the prM protein by host furin protease. Virus particles contained in vesicles are released from the cell through the exocytic pathway (Mackenzie and Westaway, 2001).

Recent studies have shown the importance of the prM protein in the maturation and secretion of virions and VLPs. Tan et al. (2009) showed that the highly conserved tyrosine at amino acid (AA) residue 78 in the ectodomain of the prM protein of WNV is essential for virus assembly and secretion from cells (Tan et al., 2009). The H99 residue in the prM protein of JEV, positioned opposite from hydrophobic surfaces on the E protein, was shown to be critical in the formation of prM-E heterodimers. The transition to neutral pH may change interactions between amino acids at this prM-E interface, leading to release of pr and formation of mature virions (Li et al., 2008). Yoshii et al. (2004) found that mutating the prM P63 to a serine greatly reduced the production of VLPs and virions of TBEV (Yoshii et al., 2004). This AA lies in the pr region of the prM protein that is conserved in flaviviruses and was shown to be crucial in the formation of prM-E heterodimers (Yoshii et al., 2012). The loss of the N-linked glycosylation site in the pr portion of JEV prM protein results in a

20-fold decrease in infectious virion production and decreased virulence in mice inoculated peripherally with mutant virus (Kim et al., 2008).

In order to map the epitope binding of 3 fully human monoclonal antibodies (hMAbs), we made four mutations (T20D, K31A, K31V, K31T) in the prM protein of the WN VLP that resulted in failure to secrete VLP antigen from transfected cells (Calvert et al., 2011). Although VLPs were not secreted as a result of these mutations, prM antigen was detected in the transfected COS-1 cells. In this report we examine the effects of these prM mutations on WN VLP assembly and secretion as well as on infectious virus replication and protein expression.

Results

Mutations in WNV prM protein affect secretion of VLP

Previously, we constructed WN VLP mutants to identify the epitopes on the prM protein recognized by 3 virus-specific hMAbs (Calvert et al., 2011). All three of the mutations made at K31 in the prM protein (K31A, K31T, K31V) resulted in significantly reduced secretion of VLP. Another mutation, T20D had the same effect on VLP secretion. These mutations occurred in AA residues that are located on the surface-exposed face of pr and did not appear to be involved in interactions with the E protein in prM-E heterodimers or disulfide bonds in the prM protein (Li et al., 2008).

To investigate the effects of these mutations on VLP secretion, COS-1 cells were transfected with WT and mutant (T20D, K31A, K31T, and K31V) pVAXWN plasmids, cell culture supernatant was harvested on days 2 and 7 post-transfection, and detection of viral proteins was performed by antigen-capture ELISA, using polyclonal rabbit serum to WNV prM and E proteins as capture antibody and mouse hyperimmune ascitic fluid (MHIAF) to WNV as detector antibody. Transfected cells were incubated at 37 °C up to 7 days. Detection of secreted prM and E proteins was reduced significantly for all prM mutants at day 2 and day 7 compared to WT using Dunnett's method of multiple comparisons with an overall type I error of 0.05 (Fig. 1). We also conducted experiments in which cells were incubated for the first 6 h at 37 °C and then transferred to 28 °C for 7 days, and similar results as those shown above were obtained (data not shown). These data indicate that K31 and to some extent T20 may play important roles in WN VLP secretion.

Effect of mutations in VLP prM on prM-E heterodimerization

During flavivirus assembly prM and E proteins form heterodimers that interact with the nucleocapsid and bud through the ER membrane to form immature virus particles. Co-expression of prM with E is necessary for correct folding of the E protein; however, prM is able to form its native structure in the absence of E protein (Konishi and Mason, 1993; Lorenz et al., 2002). To determine if the mutations in prM disrupted prM-E heterodimerization during formation of VLPs, COS-1 cells transfected with WT and prM mutant pVAXWN plasmids were lysed, prM and E proteins were immunoprecipitated with either anti-E or anti-prM MAb, and precipitated viral proteins were detected by immunoblot (Fig. 2). When VLPs were immunoprecipitated with the anti-prM hMAb 8G8, the E protein

was co-precipitated and detected in all cell lysates transfected with WT and mutant plasmids. (Fig. 2B). Interestingly, prM protein from the T20D mutant was detected as a doublet corresponding to the glycosylated and non-glycosylated forms of the protein. When VLPs were immunoprecipitated with the anti-E mMAb 3.91D, prM protein was detected in co-precipitate from lysates of cells transfected with WT and K31A, K31T and K31V mutant plasmids but apparently not with T20D mutant plasmid. When the concentration of lysate from cells transfected with T20D pVAXWN plasmid was increased 2-fold in the immunoprecipitation reaction a very small amount of non-glycosylated prM was detected (Fig. 2B). These results suggest that heterodimerization of the E and prM protein is not affected by mutations at K31, but is affected by the T20D mutation on the prM protein. The mutation at T20 permits production of both glycosylated and non-glycosylated forms of prM, and only the non-glycosylated form of the protein appears to associate with the E protein.

To confirm that the T20D mutation resulted in production of both glycosylated and non-glycosylated forms of prM, and that glycosylation of the E and prM proteins was not affected by the K31 mutations, prM and E proteins were immunoprecipitated from cell lysates and digested with the endoglycosidase, PNGaseF, which cleaves all types of N-linked of multiple glycans. The migration patterns of treated and non-treated samples were compared (Fig. 3A). The E protein from WT and prM mutants was shown to be glycosylated as indicated by an apparent shift in mobility from 54 kDa to 50 kDa. The prM proteins expressed from WT and K31 mutant plasmids were also shown to be glycosylated as indicated by a shift in mobility from 20 kDa to 17 kDa. PNGaseF digestion also confirmed that the prM doublet seen in the lysate from cells expressing the T20D mutant was due to expression of both glycosylated and non-glycosylated forms of the protein since only the smaller band (17 kDa) was visible after digestion. To determine the form of the carbohydrates on prM and E immunoprecipitated proteins were digested with endoglycosidase H (EndoH), an enzyme which cleaves the chitobiosyl unit of the high mannose form of the carbohydrate on the glycoprotein. Migration patterns of EndoH treated and untreated samples were compared (Fig. 3B). The E and prM glycoproteins of WT and mutants were shown to be sensitive to EndoH digestion indicating that in cells the glycoproteins were predominately in high mannose form. Processing of high mannose carbohydrates to the complex form takes place in the Golgi, therefore, since these protein still contained the high mannose form of the carbohydrate they must localize to the ER. The overall decrease in prM and E protein concentrations from T20D compared to WT may reflect the inability of this construct to assemble heterodimers. Since the K31 mutants expressed equal amounts of prM and E proteins in transfected cells as WT, these contructs may be able to form stable prM-E heterodimers but unable to form stable particles that can interact with cellular factors for efficient release from cells.

Mutations in WNV prM protein affect cellular localization of viral proteins

The immunoprecipitation results indicated that intracellular prM-E heterodimers are formed with the K31 prM mutants and to a much lesser extent with the T20D prM mutant, however, as shown previously, the VLPs are not secreted. Therefore, the block in secretion must occur in a later step in replication. During assembly, flaviviruses bud into the ER lumen of virus-

infected cells and are transported to the Golgi for subsequent processing (Lindenbach and Rice, 2003). To determine whether the prM mutations had an impact on the distrubution of viral proteins inside the cell, COS-1 cells transfected with WT and prM mutant pVAXWN plasmids were fixed at 6, 12, 24 and 48 h post-transfection, permeabilized and double stained with antibodies to detect E protein (mMAb 3.91D), and either ER (anti-calreticulin), coatomer (anti-βCOP I), ER-Golgi intermediate compartment (anti-ERGIC53) or Golgi (anti-GRASP65) markers (Fig. 4). At 6 h E protein expressed by WT and prM mutant plasmids coincided with ER, and ERGIC markers, with some coincidence with βCOPI and no coincidence with Golgi (data not shown). In WT transfected cells at 12 h post-transfection the distribution of the E protein completely coincided with the ER and ERGIC, and to some extent with the Golgi (Fig. 4A). At 24 h post-transfection WT E protein completely coincided with ER and ERGIC markers while moderate coincidence of E protein with the Golgi marker was observed (Fig. 4B). Staining of cells transfected with T20D mutant had simliar staining to WT. At 12 h post-transfection distrubution of the E protein completely coincided with the ER and ERGIC markers, with moderate coincidence with Golgi marker; however, unlike WT, T20D E protein also conincided with βCOPI marker (Fig. 4A). At 24 h postransfection distribution of the E protein expressed from the T20D mutant moderately coincided with ER and ERGIC markers with less coincidence with βCOPI marker and no coincidence with Golgi marker (Fig. 4B).

Distribution of the E protein expressed by the K31 mutants in transfected cells appeared to be different from WT. Moderate coincidence of E protein with βCOPI and Golgi markers and complete coincidence with ER and ERGIC markers were observed in cells transfected with K31 mutant plasmids at 12 h post-transfection (Fig. 4A). At 24 h post-transfection the E protein expressed by K31 mutants coincided with ER, ERGIC and somewhat with βCOPI markers. Staining of E protein expressed by K31 mutants and Golgi marker was not colocalized at 24 h (Fig. 4B). At 48 h E protein expressed by WT and prM mutant plasmids coincided with ER, βCOPI, and ERGIC markers. Unlike WT which did not co-localize with Golgi at 48 h, E protein expressed from K31 mutants coincided somewhat with Golgi marker (data not shown).

The most stricking result was the extremely concentrated and localized distribution of the E protein in cells expressing K31 mutants compared to the staining of the E protein from cells transfected with WT plasmid. These observations suggest that mutations at K31 in the prM protein result in an accumulation of E protein in the ER, ER–Golgi intermediary compartments and to some extent the Golgi complex, possibly due to the inability of these mutant prM-E heterodimers to effectively interact with unknown cellular factors in order to be secreted from the cell.

Effect of mutations in prM protein on virus replication

To determine if these prM VLP secretion-blocking mutations had an effect on virus maturation and release, the same mutations were introduced into an infectious cDNA clone of the WNV genome. C6/36 cells were transfected with *in vitro* transcribed, mutant WNV RNA and virus was harvested 7 days after transfection. Virus and viral RNA production were measured by plaque assay and quantitative RT-PCR (qRT-PCR). The prM and E genes

of WT and mutant virus RNA were sequenced on day 0 and day 7, and the introduced mutations were found to be present with no compensatory mutations identified. Growth characteristics of viruses were determined in one mosquito cell line (C6/36) and two mammalian cell lines (Vero and COS-1) by infecting cells at a multiplicity of infection (MOI) of 0.1 and analyzing daily medium samples by plaque assay. All 4 prM mutant viruses grew similarly to WT in C6/36 cells except for K31T, which had a titer 10-fold lower than WT virus from day 1 to day 4 (Fig. 5A). The prM mutant viruses also grew similarly to WT virus in Vero cells after day 2; however, all mutant viruses grew more slowly than WT between days 0 and 2 (Fig. 5B). Growth of the prM mutant viruses as compared to WT were most different in COS-1 cells. While K31V grew similarly to WT virus, T20D, K31A and K31T virus titers were about 10-fold lower (Fig. 5C). Average plaque sizes in Vero cells of prM mutant viruses harvested from these growth studies were compared to WT virus. No significant difference between T20D and WT plaque sizes was seen in viruses grown in any cell type. Average plaque sizes for K31A and K31T were significantly smaller compared to WT for viruses obtained from all three cell lines. The average plaque sizes were significantly less only for the K31V mutant obtained from C6/36 cells (Table 1). These results indicate that while virus growth was delayed, and plaque sizes were reduced in Vero cells compared to WT virus, the prM mutant viruses were able to overcome deleterious effects and replicate in all three cell types.

Since the prM mutants did not show significant differences from WT virus growth in all cell culture types we determined the viral RNA-to-pfu ratio of the mutants to assess the presence of defective particles and infectious virus compared to WT. Infectious virus titers in cell culture medium were determined when peak WT titer was achieved (C6/36 and COS-1 cells, day 4; Vero cells, day 2) by plaque assay, and extracellular RNA in the same samples was measured by qRT-PCR. The ratio of RNA copies/ml to PFU/ml for mutant viruses was compared to WT virus in each cell type and results are shown in Fig. 6. In C6/36 cells there was only a significant difference in the ratio of RNA copies/ml to PFU/ml for the K31V mutant compared to WT. WT virus produced 1.4 times more RNA copies/ml than PFU/ml, while the T20D, K31A, K31T and K31V mutants produced 2.4, 6.3, 7.2 and 15.4 times more RNA copies/ml than PFU/ml, respectively (Fig. 6A). None of the mutants had significantly higher ratios of RNA copies/ml than PFU/ml when compared to WT in Vero cells. WT virus produced 22 times more RNA copies/ml than PFU/ml in Vero cells, while T20D, K31A, K31T and K31V mutants produced 26, 49, 57 and 32 times more RNA copies/ml than PFU/ml, respectively (Fig. 6B). In COS-1 cells the T20D, K31T and K31V mutants had significantly higher ratios of RNA copies/ml to PFU/ml compared to WT virus. WT virus produced 15 times more RNA copies/ml than PFU/ml and T20D, K31A, K31T and K31V produced 236, 29, 45 and 51 times more RNA copies/ml than PFU/ml, respectively (Fig. 6C). These results indicate that in COS-1 cells, the T20D, K31T and K31V prM mutations resulted in less efficient production of infectious virus, and growth of the K31V mutant in C6/36 cells was less efficient in infectious virus production than WT virus.

Effect of prM mutations on hMAb binding to virions

Previously, the binding of hMAbs to WN VLP epitopes was characterized, showing that V19 and L33 were key amino acid residues in the VLP epitope recognized by all three hMAbs (Calvert et al., 2011). Since the prM mutations (T20D, K31A, K31T and K31V) prevented secretion of VLP, binding could not be tested in ELISA. Therefore, these mutations, along with 9 other mutations (V19A, V19N, V19T, T20A, T20Q, T24A, L33A, L33K, L33Q) in the pr peptide found to have significant effects on hMAb binding, were incorporated into the WNV infectious cDNA clone (Calvert et al., 2011). *In vitro*-transcribed RNA was transfected into C6/36 cells, and virus was harvested 7 days later. Introduced mutations were confirmed by sequencing of the prM and E genes, and virus titer was determined by plaque assay. COS-1 cells were infected with all prM mutant WNVs at an MOI of 0.1 to produce virus for antigen-capture ELISA to test hMAb binding. COS-1 derived virus was used in the assay in order to directly compare hMAb binding to previous results with VLPs secreted from transfected COS-1 cells. Human sera positive for anti-flavivirus antibody was used as a control in the ELISA to validate that the concentrations of viral proteins were uniform for all mutant viruses tested. Fold changes in reactivity with the control sera range from 0 to 2 and indicate that virus preps used in the ELISA contained comparative concentrations of viral proteins.

The only mutations that resulted in a significant reduction in reactivity with hMAb 8G8 were K31A and K31V, with 5- and 4-fold reductions of end-point titers, respectively. The T20D mutation resulted in a 10-fold increase in reactivity with hMAb 8G8. All other mutations in the pr peptide of WNV resulted in 3-fold or less reduction in hMAb end-point titers, which was not considered significant (Table 2). These results suggest that the K31 AA residue in virion prM may be important in the binding of hMAb 8G8.

Discussion

Recent research on the functional importance of the prM protein in flavivirus infections has revealed that the protein is not only important for viral structure and assembly, but also plays an important role in infection and immunity. New evidence shows that non-neutralizing antibodies to prM can enhance DENV infection of Fc receptor-bearing cells *in vitro* as well as enhance WNV infection *in vivo* (Colpitts et al., 2011; Huang et al., 2008, 2006). These anti-prM antibodies may assist immature virus particles in cell entry, thereby increasing the number of virus-producing cells in secondary infections (Dejnirattisai et al., 2010; Rodenhuis-Zybert et al., 2010). The prM protein of flaviviruses also plays an important role as a chaperone to the major envelope glycoprotein E. Not only is the prM protein required for proper folding and maturation of the E protein during virus assembly, it also protects the fusion loop on the E protein from premature fusion before exiting the cell (Konishi and Mason, 1993; Lorenz et al., 2002; Yu et al., 2009). Recently, the prM protein of DENV has been shown to associate with members of the ADP-ribosylation factor (Arf) family of proteins (Kudelko et al., 2012; Wang et al., 2009). These host cellular factors are known to play a critical role in intracellular trafficking as well as modulating membrane curvature, a function critical to the assembly and budding of flaviviruses from the ER membrane (Beck et al., 2008; Garoff et al., 1998). The prM protein of DENV was also shown to interact with

vacuolar-ATPases (V-ATPases) in infected cells. These enzymes acidify intracellular organelles, including those in the secretory pathway, and pump protons across the plasma membrane of the cell. This interaction could be significant in both virus entry and membrane fusion via acidified endosomes and secretion of newly assembled virus particles out of the cell (Duan et al., 2008).

In the present study, we describe the effects of 4 specific mutations in the WNV prM protein on WN VLP secretion. Mutations made in prM K31 and T20 in the prM expressed from the pVAXWN plasmid resulted in a loss of VLP secretion from transfected COS-1 cells. While K31 mutants were shown to efficiently form prM-E heterodimers, VLP particle secretion was blocked, resulting in accumulation of viral proteins in the ER, ER–Golgi intermediary compartments and to some extent in the Golgi of transfected cells.

Assembly and maturation of viral particles begins at the membrane of the ER. The prM and E proteins dimerize and then form an icosahedral scaffold that leads to budding of the enveloped particles into the lumen of the ER. These virus particles are transported through the Golgi and released from the cell via the exocytic pathway; however, the exact details of this process are poorly characterized (Mackenzie and Westaway, 2001; Welsch et al., 2009). Flaviviruses have been shown to associate with calnexin and calreticulin, lectins found in the ER that assist in the proper folding of glycoproteins, chaperoning them through the ER and retaining incompletely folded proteins (Courageot et al., 2000; Lorenz et al., 2003; Mackenzie and Westaway, 2001; Wu et al., 2002). Arf proteins have been implicated in DENV VLP trafficking from the ER to the Golgi since depletion of Arf1, Arf4 and Arf5 resulted in blocking secretion of VLPs and virions (Kudelko et al., 2012; Wang et al., 2009). In fact, the prM protein was found to interact with these cellular factors, which may be crucial in the trafficking and secretion of virus particles through the cell. While all four DENVs and YFV were shown to produce less virus when these proteins were down-regulated in the infected cell, this had no effect on WNV infection and secretion (Kudelko et al., 2012). This descrepancy may be due to differences in the two viral particle systems studied, or it may be due to an inconsistency of the role of these cellular proteins in flavivirus maturation and secretion.

Interestingly, the epitope containing K31 in the prM protein is positioned at the top of the prM-E trimer spike in immature virus particles (Fig. 7A). These mutations had no effect on prM-E heterodimer formation and protein glycosylation, and appear to play no role in stabilization of trimer spike formation. Since its role in virus assembly does not appear to be structurally-related, we can hypothesize that it must play some role in interacting with host cellular factors in trafficking the particles through the ER, Golgi and ultimately out of the cell. L33 was previously mutated in the WN VLP to an alanine, lysine, glutamine and threonine and had no effect on VLP secretion (Calvert et al., 2011). This epitope is not positioned as prominently on the top of the prM-E trimer spike as K31 (Figs. 7A and B). It is also interesting that the K31 AA residue is sandwiched between two highly conserved residues among flaviviruses, G30 and N32, which may indicate that this region of prM plays some critical role for prM structure and function.

The T20D mutation in the prM protein resulted in failure to form the prM-E heterodimer containing glycosylated prM as shown by immunoprecipitation studies of lysates from cells transfected with the mutated plasmid. The T20D mutation caused inefficient glycosylation of the prM protein, and interestingly only small amounts of non-glycosylated T20D prM were shown to associate with the E protein (Fig. 2B). The plasmid with T20D mutation also expressed glycosylated prM in COS-1, but they were not associated with E protein. Glycosylation of the E protein of flaviviruses has been studied extensively and shown to be a critical factor in flavivirus replication, maturation and neuroinvasiveness in mice (Beasley et al., 2005b; Lad et al., 2000; Li et al., 2006; Scherret et al., 2001). Glycosylation of the prM protein has also been shown to be important for heterodimer formation and secretion of viral proteins from the cell. In JEV, glycosylation of the prM protein was shown to be an important factor in virion assembly and release as well as viral pathogenicity in mice (Kim et al., 2008). Deletion of the prM glycosylation site resulted in a reduction of secreted TBE and WN VLPs (Goto et al., 2005; Hanna et al., 2005). The T20 AA residue lies in close proximity to the glycosylation site on the prM protein in WNV at N15-X16-T17 (Fig. 7B). While the mutation does not directly affect the sequence of the glycosylation site, mutating the small hydrophilic AA residue threonine to a large negatively charged AA residue aspartic acid could affect the local biochemistry of the region which in turn could prevent effective glycosylation of the prM in the heterodimer structure and/or destabilize heterodimers containing the glycosylated T20D prM. Likewise, each of the prM-E heterodimers may be affected by the T20 residues in the other two prM proteins in close proximity in the prM-E trimer spike (Fig. 7B). Previously, mutations made at this AA residue (A, G, Q) and those made at AA residue V19 (A, N, R, T) had no effect on VLP secretion (Calvert et al., 2011).

While these mutations had significant effects on VLP secretion, their effect on virus replication was measurable, but not as dramatic. K31 mutants replicated reasonably well in the three cell types tested (C6/36, COS-1 and Vero cells), with a few exceptions. The K31T mutant replicated more slowly in C6/36 cells than WT or the other prM mutant viruses, while in Vero cells all the mutants replicated more slowly than WT before day 2 post-infection. In contrast, K31V was the only mutant to replicate similarly to WT virus in COS-1 cells. Comparisons of plaque morphology revealed that all K31 mutants obtained from any of the three cell types (except for K31V from COS-1 cells) produced significantly smaller plaques than WT viruses in Vero cells, indicating a replication defect. In comparisons of the amount of extracellular virus RNA (presumably packaged in defective particles) to infectious virus particles, the K31V mutant produced significantly higher ratios of RNA to infectious virus than WT virus in C6/36 and COS-1 cells, while the K31T mutant only produced significantly higher ratios of RNA to infectious virus than WT virus in COS-1 cells. The T20D mutant also produced higher ratios of RNA to virus than WT virus in COS-1 cells. While the differences in production of VLP and virus particles with these mutations are surprising, it is not unprecedented. TBE VLP secretion was inhibited by a mutation at prM AA residue 63 from a proline to a serine; however, when this same mutation was incorporated into the virus genome, only a 10-fold decrease in titer over the first 48 h of replication was documented (Yoshii et al., 2004). Likewise, when mutations in JEV ablated glycosylation of the prM protein, virus particles continued to be produced,

although at a 20-fold decreased titer from WT (Kim et al., 2008). Taken together, these studies demonstrate that mutations that affect VLP formation and secretion may not completely have the same effects on virions. This observation is important to consider when using VLPs to study virus structure and function, and significant findings should be confirmed with replicating virus.

Epitope mapping with hMAbs to the WNV WT and mutant prM proteins revealed a large disparity between VLP and virion presentation of the prM protein. This may be due to the relative concentrations of prM present in the two systems, or to the presentation of the protein itself and the accessibility of the epitopes recognized by these hMAbs. Concentrations of VLPs were standardized by optical density in an ELISA designed to detect all prM and E proteins in the supernatant. Virions were standardized by PFU/ml titers, and viral protein concentrations were validated with the inclusion of polyclonal anti-flavivirus human sera. TBE VLP which only contains M is the only VLP structure to be solved of the flaviviruses, therefore it is difficult to compare the unknown structure of the WN VLP with the resolved structure of the mature and immature flavivirus particle (Ferlenghi et al., 2001; Kuhn et al., 2002; Zhang et al., 2003). While differences between virus- and VLP-expressed E protein do not appear to affect epitope expression, differences in protein arrangements between VLP, mature and immature virions could account for differences in epitope recognition on the prM protein by the hMAbs in our study. We are currently conducting co-crystallization studies to elucidate binding of virions by hMAbs.

This study reiterates the importance of the prM protein in maturation and assembly of VLP and virions and highlights a structural region that has not been previously shown to be important for particle maturation and secretion. The K31 AA residue in the prM protein of WNV has a significant impact on WNV particle assembly and secretion processes. Further investigation into the specific role of the prM protein and the critical epitopes involved will be needed to understand the process of intracellular trafficking of virus.

Materials and methods

Cells

C6/36 (*Aedes albopictus* mosquito), Vero (African green monkey kidney) and COS-1 (African green monkey kidney) cells were cultured as described previously (Davis et al., 2001; Huang et al., 2000). Cells were maintained in DMEM (Invitrogen) supplemented with 10% fetal bovine serum (FBS), 2 mM L-glutamine, 110 mg/L sodium pyruvate, 0.1 mM nonessential amino acids, 20 ml/L 7.5% sodium bicarbonate and penicillin (100 U/ml)/ streptomycin (100 μg/ml). Vero and COS-1 cells were grown at 37 °C with 5% CO_2 while C6/36 cells were grown at 28 °C with5% CO_2.

Antibodies

The anti-prM MAbs 8G8 and 5G12 (a kind gift from I. Trakht and G. Kalantarov, Columbia University) are WNV specific hMAbs reacting to AA residues V19 and L33 in the prM protein of the VLP (Calvert et al., 2011). Anti-E MAbs 3.91D and 3.67G were obtained from the Arbovirus Diagnostic and Reference Collection activity, DVBD/ADB. These MAbs

used in the immunoprecipitation studies are WNV specific mMAbs reacting to AA residues S306, K307 and T332 in DIII of the E protein (David C. Clark, unpublished data).

Site-directed mutagenesis and production of mutant infectious WNV and WN VLP

The WNV two-plasmid infectious clone (WN-IC) and pVAXWN plasmid were utilized to produce WNV and VLP respectively, as previously described (Beasley et al., 2005a; Davis et al., 2001; Kinney et al., 2006). Site-specific mutations were introduced into the prM gene of both systems using the QuikChange site-directed mutagenesis kit (Stratagene). Mutagenic primer sequences used for all constructs and transient expression of WN VLP in COS-1 cells by pVAXWN electroporation have been previously described (Calvert et al., 2011). Electroporated COS-1 cells were recovered in 6 ml of DMEM supplemented with 10% FCS. Cells were seeded into 25-cm^2 culture flasks for VLP expression and incubated at 37 °C with 5% CO2. Six hours after electroporation, the growth medium in flasks was replaced with DMEM containing 2% FCS. Tissue culture medium were harvested 2 and 7 days after electroporation for determination of VLP secretion by ELISA.

Once full length WN-IC cDNA was obtained, *in vitro* transcription of RNA was carried out as previously described (Kinney et al., 2006). C6/36 cells were transfected with transcribed RNA by electroporation. Transfected cells were incubated at 28 °C/5% CO_2 for 7 days at which point supernatant was harvested and infectious virus titers were determined by plaque assay. The prM and E genes of WT and mutant viruses were sequenced, and the correct mutations were found to be present in all mutant viruses with no compensatory mutations present.

Characterization of WN-IC mutant viruses in culture

Viral growth curves were performed in triplicate in 6 well plates of Vero, COS-1 or C6/36 cells at a MOI of 0.1. After adsorption for 1 h, maintenance medium containing 2% FCS and penicillin/streptomycin was added and cultures were incubated in 5% CO_2 at 37 °C (Vero and COS-1 cells) or 28 °C (C636 cells). Aliquots of culture medium were harvested every day for 7 days, FCS concentration was adjusted to 20% and aliquots were stored at 80 °C prior to titration and RNA extraction. Viral RNA was extracted from virus supernatant with a QIAmp Viral RNA kit (Qiagen). WNV-specific primers to the structural genes used were based on published data of WNV, strain NY99, and sequencing was carried out as previously described (Kinney et al., 2006). Viral RNA was also quantitated at peak viral titers on either day 2 for Vero or day 4 for COS-1 and C6/36 cells. A 5 μl aliquot of each sample was added to master mix from iScript One-step RT-PCR kit (Bio-Rad) containing 200 nM of probe, WN1186F (5′–FAM-TGC CCG ACC ATG GGA GAA GCT C–3′), 200 nM of forward primer, WN1160 (5′–TCA GCG ATC TCT CCA CCA AAG–3′) and 200 nM of reverse primer, cWN1229 (5′–GGG TCA GCA CGT TTG TCA TTG-3′). WNV-specific RNA was tested in triplicate and measured by qRT-PCR using homologous RNA standards on a Bio-Rad IQ5 Real-time PCR detection system under the following conditions: 50 °C for 30 min, 95 °C for 15 min, followed by 45 cycles of 94 °C for 15 s, and 57 °C for 1 min with continuous fluorescence data collection. Virus plaque titrations were performed under double agarose overlay in six-well plates of confluent Vero cells (Huang et al., 2000). The

second agarose overlay containing neutral red vital stain was added 4 days after infection, and plaques were counted on day 5 after infection.

Analysis of intracellular mutant VLP proteins

Two days after transfection of COS-1 cells with pVAXWN WT and mutant plasmids, cells were harvested and cell lysate was produced as previously described (Blitvich et al., 2003). Similarly, control antigen was produced with non-transfected COS-1 cells. Viral proteins were immunoprecipitated from lysates using the Pierce Immunoprecipitation kit (Thermo Scientific) with resin coupled to 75 μg of WNV murine anti-E 3.91D antibody or 75 μg of WNV human anti-prM 8G8 antibody following the manufacturer's in lysates were analyzed by digestion after immunoprecipitation using *N*-glycosidase F (PNGaseF) or Endoglycosidase H (EndoH) (New England Biolabs) following the manufacturer's protocol, before analysis by SDS-PAGE.

SDS-PAGE and immunoblotting

WN viral proteins from immunoprecipitated lysates were separated by SDS-PAGE on a reduced 4–12% Bis/Tris gel (Invitro-gen). All procedures were performed at room temperature. Proteins were blotted electrophoretically from the gels onto nitrocellulose membranes and washed for 5 min in PBS/0.1% Tween wash buffer. Non-specific binding sites were blocked with 1% BSA/PBS for 1 h while rocking. WNV murine anti-E MAb, 3.67 G (10 μg), and purified rabbit polyclonal sera to WNV prM (10 μg) (Meridian LifeScience) were incubated with the membrane for 1 h with gentle rocking. Membranes were washed again in PBS/0.1% Tween wash buffer three times for 5 min each. Goat anti-mouse antibody and goat anti-rabbit antibody conjugated to alkaline phosphatase (Jackson Immunoresearch) were diluted 1:200 and incubated on the membrane for 1 h with gentle rocking. Membranes were washed as described previously and BCIP/NBT phosphatase substrate (KPL) was added to the membrane until a color change appeared. The reaction was stopped by the addition of water.

ELISAs

All ELISAs were performed in 96-well plates (Maxisorp plates, Nunc). To test for secretion of mutant VLP antigen, rabbit hyperimmune sera to WNV prM and E proteins was diluted 1:1000 in carbonate/bicarbonate buffer (50 mM sodium carbonate, 50 mM sodium bicarbonate, pH 9.6) and incubated overnight at 4 °C. Plates were washed five times with PBS/0.1% Tween wash buffer with an automatic plate washer. Non-specific binding sites were blocked with 3% rabbit serum in PBS (100 μl/well) and incubated at 37 °C for 1 h. Blocking buffer was removed before supernatant from transfected COS-1 cells was added to the plate in doubling dilutions in 3% rabbit serum/PBS (50 μl/well). Antigen was incubated at 37 °C for 2 h, after which the plates were washed as previously described. MHIAF to WNV was obtained from the Reference Collection of the Diagnostic Laboratory, ADB, DVBID, CDC, and used as the primary antibody at a dilution of 1:1600 in 3% rabbit serum/PBS and incubated at 37 °C for 1 h. Plates were washed 5 times before the addition of rabbit anti-mouse antibody conjugated to horseradish peroxidase (50 μl/well), diluted 1:5000 in 3% rabbit serum/PBS. After an incubation period of 1 h at 37 °C, plates were washed again ten times. Enhanced K-blue TMB substrate (Neogen) was added to each well of the

plate (100 μl/well) and incubated in the dark at room temperature for 10 min. The reaction was stopped with the addition of 1 N H_2SO_4 (50 μl/well), and the plates were read at 450 nm on an automatic plate reader.

To test the reactivity of the mutant viruses with the hMAbs the protocol remained the same with some exceptions. Viruses were diluted to a concentration of 10^6 PFU/ml in 3% rabbit serum/PBS. Purified hMAbs were used as the primary antibody and added to the wells in two-fold dilutions in 3% rabbit serum/PBS (50 μl/well) starting at 50 μg/ml. The secondary MAb, rabbit anti-human conjugated to horseradish peroxidase (50 μl/well) was diluted 1:5000 in 3% rabbit serum/PBS. The rest of the ELISA was carried out as described above.

Immunofluorescence and confocal microscopy

Transfected COS-1 cells were grown on 8-well chamber slides (Labtek) and incubated in 5% CO_2 at 37 °C. 48 h after transfection, medium was removed and cells were washed 3 times in PBS. Cells were fixed to the slide with 4% (w/v) paraformaldehyde in PBS for 10 min and permeabilized with 0.1% (v/v) Triton-X 100 in 0.2% (w/v) BSA/PBS for 10 min. Non-specific sites were blocked with 10% (v/v) goat serum in PBS for 30 min at 37 °C. Cells were incubated with WNV murine anti-E antibody 3.91D (5 μg/ml) and either rabbit anti-calreticulin (1:500), rabbit anti-βCOP1 (1:100), rabbit anti-ERGIC53 (1:100) or rabbit anti-GRASP65 (1:500) diluted in PBS for 30 min at 37 °C before being washed 3 times in PBS. Secondary antibodies, goat anti-mouse conjugated to FITC and goat anti-rabbit conjugated to Texas Red, were diluted 1:100 in PBS and incubated on the cells for 30 min at 37 °C, and cells were washed again as previously described. Slides were dried before the addition of Prolong Gold anti-fade reagent with DAPI (Invitrogen). Coverslips were mounted on the slides and allowed to cure at room temperature overnight. Images were viewed and collected with a Carl Zeiss LSM-Pascal confocal microscope.

Acknowledgments

We thank Dr. Gwong-Jen J. Chang (U.S. Centers for Disease Control and Prevention, Fort Collins, CO, USA) for providing the pVAXWN plasmid, Dr. Gary Kalantarov and Dr. Ilya Trakht (Columbia University, New York, NY, USA) for the use of hMAbs 8G8 and 5G12 and Dr. Mark Delorey for statistical analysis.

References

Beasley DW, Whiteman MC, Zhang S, Huang CY, Schneider BS, Smith DR, Gromowski GD, Higgs S, Kinney RM, Barrett AD. Envelope protein glycosylation status influences mouse neuroinvasion phenotype of genetic lineage 1 West Nile virus strains. J. Virol. 2005a; 79(13):8339–8347. [PubMed: 15956579]

Beasley DWC, Whiteman MC, Zhang SL, Huang CYH, Schneider BS, Smith DR, Gromowski GD, Higgs S, Kinney RM, Barrett ADT. Envelope protein glycosylation status influences mouse neuroinvasion phenotype of genetic lineage 1 West Nile Virus strains. J. Virol. 2005b; 79(13):8339–8347. [PubMed: 15956579]

Beck R, Sun Z, Adolf F, Rutz C, Bassler J, Wild K, Sinning I, Hurt E, Brugger B, Bethune J, Wieland F. Membrane curvature induced by Arf1-GTP is essential for vesicle formation. Proc. Natl. Acad. Sci. USA. 2008; 105(33):11731–11736. [PubMed: 18689681]

Blitvich BJ, Marlenee NL, Hall RA, Calisher CH, Bowen RA, Roehrig JT, Komar N, Langevin SA, Beaty BJ. Epitope-blocking enzyme-linked immunosorbent assays for the detection of serum antibodies to west nile virus in multiple avian species. J. Clin. Microbiol. 2003; 41(3):1041–1047. [PubMed: 12624027]

Calvert AE, Kalantarov GF, Chang GJ, Trakht I, Blair CD, Roehrig JT. Human monoclonal antibodies to West Nile virus identify epitopes on the prM protein. Virology. 2011; 410(1):30–37. [PubMed: 21084104]

Cherrier MV, Kaufmann B, Nybakken GE, Lok SM, Warren JT, Chen BR, Nelson CA, Kostyuchenko VA, Holdaway HA, Chipman PR, Kuhn RJ, Diamond MS, Rossmann MG, Fremont DH. Structural basis for the preferential recognition of immature flaviviruses by a fusion-loop antibody. EMBO J. 2009; 28(20):3269–3276. [PubMed: 19713934]

Colpitts TM, Rodenhuis-Zybert I, Moesker B, Wang P, Fikrig E, Smit JM. prM-antibody renders immature West Nile virus infectious *in vivo*. J. Gen. Virol. 2011; 92(Part 10):2281–2285. [PubMed: 21697345]

Courageot MP, Frenkiel MP, Dos Santos CD, Deubel V, Despres P. Alpha-glucosidase inhibitors reduce dengue virus production by affecting the initial steps of virion morphogenesis in the endoplasmic reticulum. J. Virol. 2000; 74(1):564–572. [PubMed: 10590151]

Davis BS, Chang GJ, Cropp B, Roehrig JT, Martin DA, Mitchell CJ, Bowen R, Bunning ML. West Nile virus recombinant DNA vaccine protects mouse and horse from virus challenge and expresses *in vitro* a noninfectious recombinant antigen that can be used in enzyme-linked immunosorbent assays. J. Virol. 2001; 75(9):4040–4047. [PubMed: 11287553]

Davis CW, Nguyen HY, Hanna SL, Sanchez MD, Doms RW, Pierson TC. West Nile virus discriminates between DC-SIGN and DC-SIGNR for cellular attachment and infection. J. Virol. 2006; 80(3):1290–1301. [PubMed: 16415006]

Dejnirattisai W, Jumnainsong A, Onsirisakul N, Fitton P, Vasanawathana S, Limpitikul W, Puttikhunt C, Edwards C, Duangchinda T, Supasa S, Chawansuntati K, Malasit P, Mongkolsapaya J, Screaton G. Cross-reacting antibodies enhance dengue virus infection in humans. Science. 2010; 328(5979): 745–748. [PubMed: 20448183]

Duan X, Lu X, Li J, Liu Y. Novel binding between pre-membrane protein and vacuolar ATPase is required for efficient dengue virus secretion. Biochem. Biophys. Res. Commun. 2008; 373(2): 319–324. [PubMed: 18573235]

Ferlenghi I, Clarke M, Ruttan T, Allison SL, Schalich J, Heinz FX, Harrison SC, Rey FA, Fuller SD. Molecular organization of a recombinant subviral particle from tick-borne encephalitis virus. Mol. Cell. 2001; 7(3):593–602. [PubMed: 11463384]

Garoff H, Hewson R, Opstelten DJ. Virus maturation by budding. Microbiol. Mol. Biol. Rev. 1998; 62(4):1171–1190. [PubMed: 9841669]

Goto A, Yoshii K, Obara M, Ueki T, Mizutani T, Kariwa H, Takashima I. Role of the N-linked glycans of the prM and E envelope proteins in tick-borne encephalitis virus particle secretion. Vaccine. 2005; 23(23):3043–3052. [PubMed: 15811651]

Guirakhoo F, Bolin RA, Roehrig JT. The Murray Valley encephalitis virus prM protein confers acid resistance to virus particles and alters the expression of epitopes within the R2 domain of E glycoprotein. Virology. 1992; 191(2):921–931. [PubMed: 1280384]

Hanna SL, Pierson TC, Sanchez MD, Ahmed AA, Murtadha MM, Doms RW. N-linked glycosylation of west nile virus envelope proteins influences particle assembly and infectivity. J. Virol. 2005; 79(21):13262–13274. [PubMed: 16227249]

Huang CY, Butrapet S, Pierro DJ, Chang GJ, Hunt AR, Bhamarapravati N, Gubler DJ, Kinney RM. Chimeric dengue type 2 (vaccine strain PDK-53)/dengue type 1 virus as a potential candidate dengue type 1 virus vaccine. J. Virol. 2000; 74(7):3020–3028. [PubMed: 10708416]

Huang KC, Lee MC, Wu CW, Huang KJ, Lei HY, Cheng JW. Solution structure and neutralizing antibody binding studies of domain III of the dengue-2 virus envelope protein. Proteins. 2008; 70(3):1116–1119. [PubMed: 18004779]

Huang KJ, Yang YC, Lin YS, Huang JH, Liu HS, Yeh TM, Chen SH, Liu CC, Lei HY. The dual-specific binding of dengue virus and target cells for the antibody-dependent enhancement of dengue virus infection. J. Immunol. 2006; 176(5):2825–2832. [PubMed: 16493039]

Junjhon J, Edwards TJ, Utaipat U, Bowman VD, Holdaway HA, Zhang W, Keelapang P, Puttikhunt C, Perera R, Chipman PR, Kasinrerk W, Malasit P, Kuhn RJ, Sittisombut N. Influence of pr-M cleavage on the heterogeneity of extracellular dengue virus particles. J. Virol. 2010; 84(16):8353–8358. [PubMed: 20519400]

Kim JM, Yun SI, Song BH, Hahn YS, Lee CH, Oh HW, Lee YM. A single N-linked glycosylation site in the Japanese encephalitis virus prM protein is critical for cell type-specific prM protein biogenesis, virus particle release, and pathogenicity in mice. J. Virol. 2008; 82(16):7846–7862. [PubMed: 18524814]

Kinney RM, Huang CY, Whiteman MC, Bowen RA, Langevin SA, Miller BR, Brault AC. Avian virulence and thermostable replication of the North American strain of West Nile virus. J. Gen. Virol. 2006; 87(Part 12):3611–3622. [PubMed: 17098976]

Konishi E, Mason PW. Proper maturation of the Japanese encephalitis virus envelope glycoprotein requires cosynthesis with the premembrane protein. J. Virol. 1993; 67(3):1672–1675. [PubMed: 8437237]

Konishi E, Pincus S, Paoletti E, Shope RE, Burrage T, Mason PW. Mice immunized with a subviral particle containing the Japanese encephalitis virus prM/M and E proteins are protected from lethal JEV infection. Virology. 1992; 188(2):714–720. [PubMed: 1585642]

Kudelko M, Brault JB, Kwok K, Li MY, Pardigon N, Peiris JS, Bruzzone R, Despres P, Nal B, Wang PG. Class II ADP-ribosylation factors are required for efficient secretion of dengue viruses. J. Biol. Chem. 2012; 287(1):767–777. [PubMed: 22105072]

Kuhn RJ, Zhang W, Rossmann MG, Pletnev SV, Corver J, Lenches E, Jones CT, Mukhopadhyay S, Chipman PR, Strauss EG, Baker TS, Strauss JH. Structure of dengue virus: implications for flavivirus organization, maturation, and fusion. Cell. 2002; 108(5):717–725. [PubMed: 11893341]

Lad VJ, Shende VR, Gupta AK, Koshy AA, Roy A. Effect of tunicamycin on expression of epitopes on Japanese encephalitis virus glycoprotein E in porcine kidney cells. Acta Virol. 2000; 44(6): 359–364. [PubMed: 11332279]

Li J, Bhuvanakantham R, Howe J, Ng ML. The glycosylation site in the envelope protein of West Nile virus (Sarafend) plays an important role in replication and maturation processes. J. Gen. Virol. 2006; 87(Part 3):613–622. [PubMed: 16476982]

Li L, Lok SM, Yu IM, Zhang Y, Kuhn RJ, Chen J, Rossmann MG. The flavivirus precursor membrane-envelope protein complex: structure and maturation. Science. 2008; 319(5871):1830–1834. [PubMed: 18369147]

Lindenbach BD, Rice CM. Molecular biology of flaviviruses. Adv. Virus Res. 2003; 59:23–61. [PubMed: 14696326]

Lorenz IC, Allison SL, Heinz FX, Helenius A. Folding and dimerization of tick-borne encephalitis virus envelope proteins prM and E in the endoplasmic reticulum. J. Virol. 2002; 76(11):5480–5491. [PubMed: 11991976]

Lorenz IC, Kartenbeck J, Mezzacasa A, Allison SL, Heinz FX, Helenius A. Intracellular assembly and secretion of recombinant subviral particles from tick-borne encephalitis virus. J. Virol. 2003; 77(7):4370–4382. [PubMed: 12634393]

Mackenzie JM, Westaway EG. Assembly and maturation of the flavivirus Kunjin virus appear to occur in the rough endoplasmic reticulum and along the secretory pathway, respectively. J. Virol. 2001; 75(22):10787–10799. [PubMed: 11602720]

Mackenzie JS, Gubler DJ, Petersen LR. Emerging flaviviruses: the spread and resurgence of Japanese encephalitis, West Nile and dengue viruses. Nat. Med. 2004; 10(12 Suppl):S98–109. [PubMed: 15577938]

Nelson S, Jost CA, Xu Q, Ess J, Martin JE, Oliphant T, Whitehead SS, Durbin AP, Graham BS, Diamond MS, Pierson TC. Maturation of West Nile virus modulates sensitivity to antibody-mediated neutralization. PLoS Pathog. 2008; 4(5):e1000060. [PubMed: 18464894]

Pokidysheva E, Zhang Y, Battisti AJ, Bator-Kelly CM, Chipman PR, Xiao C, Gregorio GG, Hendrickson WA, Kuhn RJ, Rossmann MG. Cryo-EM reconstruction of dengue virus in complex with the carbohydrate recognition domain of DC-SIGN. Cell. 2006; 124(3):485–493. [PubMed: 16469696]

Rodenhuis-Zybert IA, van der Schaar HM, da Silva Voorham JM, van der Ende-Metselaar H, Lei HY, Wilschut J, Smit JM. Immature dengue virus: a veiled pathogen? PLoS Pathog. 2010; 6(1):e1000718. [PubMed: 20062797]

Schalich J, Allison SL, Stiasny K, Mandl CW, Kunz C, Heinz FX. Recombinant subviral particles from tick-borne encephalitis virus are fusogenic and provide a model system for studying flavivirus envelope glycoprotein functions. J. Virol. 1996; 70(7):4549–4557. [PubMed: 8676481]

Scherret JH, Mackenzie JS, Khromykh AA, Hall RA. Biological significance of glycosylation of the envelope protein of Kunjin virus. Ann. N. Y. Acad. Sci. 2001; 951:361–363. [PubMed: 11797800]

Tan TT, Bhuvanakantham R, Li J, Howe J, Ng ML. Tyrosine 78 of premembrane protein is essential for assembly of West Nile virus. J. Gen. Virol. 2009; 90(Part 5):1081–1092. [PubMed: 19264649]

Wang PG, Kudelko M, Lo J, Siu LY, Kwok KT, Sachse M, Nicholls JM, Bruzzone R, Altmeyer RM, Nal B. Efficient assembly and secretion of recombinant subviral particles of the four dengue serotypes using native prM and E proteins. PLoS One. 2009; 4(12):e8325. [PubMed: 20016834]

Welsch S, Miller S, Romero-Brey I, Merz A, Bleck CK, Walther P, Fuller SD, Antony C, Krijnse-Locker J, Bartenschlager R. Composition and three-dimensional architecture of the dengue virus replication and assembly sites. Cell Host Microbe. 2009; 5(4):365–375. [PubMed: 19380115]

Wu SF, Lee CJ, Liao CL, Dwek RA, Zitzmann N, Lin YL. Antiviral effects of an iminosugar derivative on flavivirus infections. J. Virol. 2002; 76(8):3596–3604. [PubMed: 11907199]

Yoshii K, Igarashi M, Ichii O, Yokozawa K, Ito K, Kariwa H, Takashima I. A conserved region in the prM protein is a critical determinant in the assembly of flavivirus particles. J. Gen. Virol. 2012; 93(Part 1):27–38. [PubMed: 21957123]

Yoshii K, Konno A, Goto A, Nio J, Obara M, Ueki T, Hayasaka D, Mizutani T, Kariwa H, Takashima I. Single point mutaton in tick-borne encephalitis virus prM protein induces a reduction of virus particle secretion. J. Gen. Virol. 2004; 85(Part 10):3049–3058. [PubMed: 15448368]

Yu IM, Holdaway HA, Chipman PR, Kuhn RJ, Rossmann MG, Chen J. Association of the pr peptides with dengue virus at acidic pH blocks membrane fusion. J. Virol. 2009; 83(23):12101–12107. [PubMed: 19759134]

Zhang Y, Corver J, Chipman PR, Zhang W, Pletnev SV, Sedlak D, Baker TS, Strauss JH, Kuhn RJ, Rossmann MG. Structures of immature flavivirus particles. EMBO J. 2003; 22(11):2604–2613. [PubMed: 12773377]

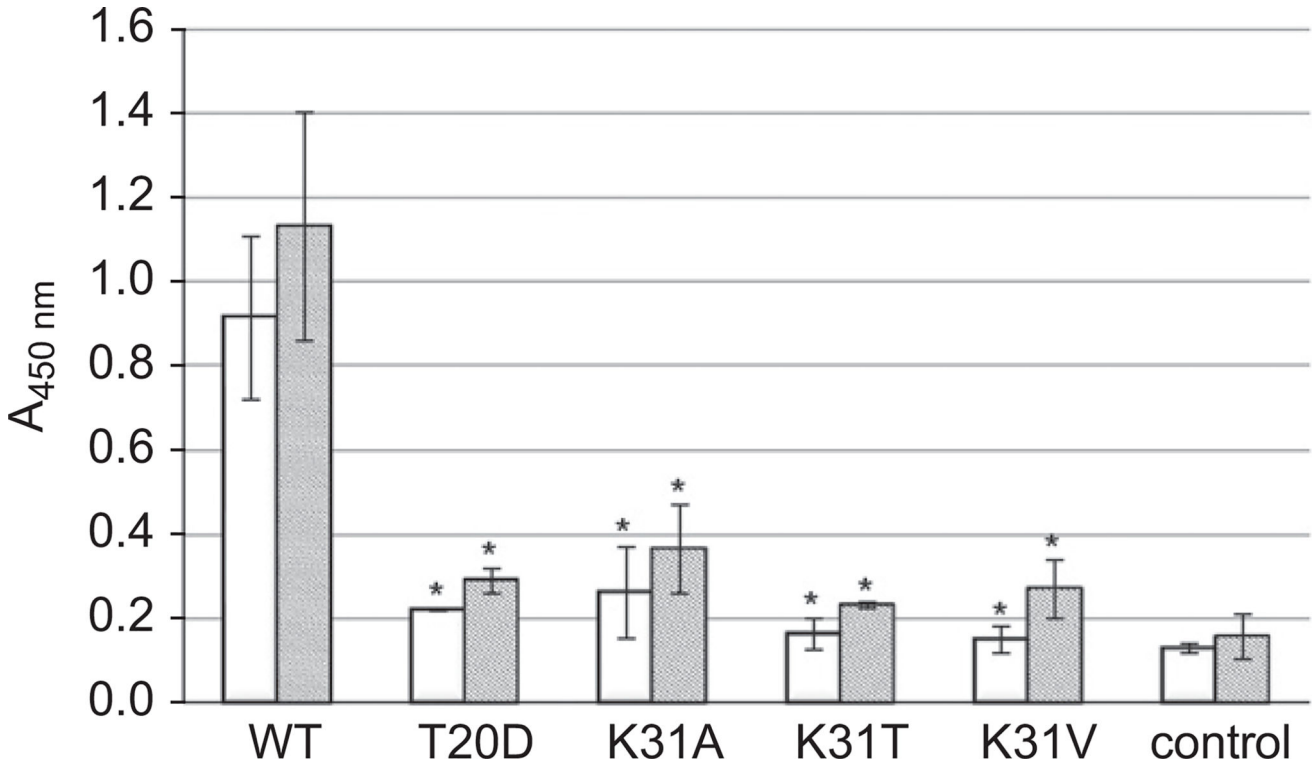

Fig. 1.

Mutations in the prM protein reduce secretion of VLPs. COS-1 cells were transfected with wild type (WT) and mutant pVAXWN plasmids. Cell culture supernatant was harvested 2 (open bars) and 7 (cross-hatched bars) days post-transfection, and prM and E proteins were detected by ELISA. Mean absorbance values (±SE) were calculated from two independent experiments performed in duplicate. Asterisks indicate statistically significant differences compared to WT plasmid using Dunnett's method of multiple comparisons with an overall type I error of 0.05. Control, non-transfected cell control.

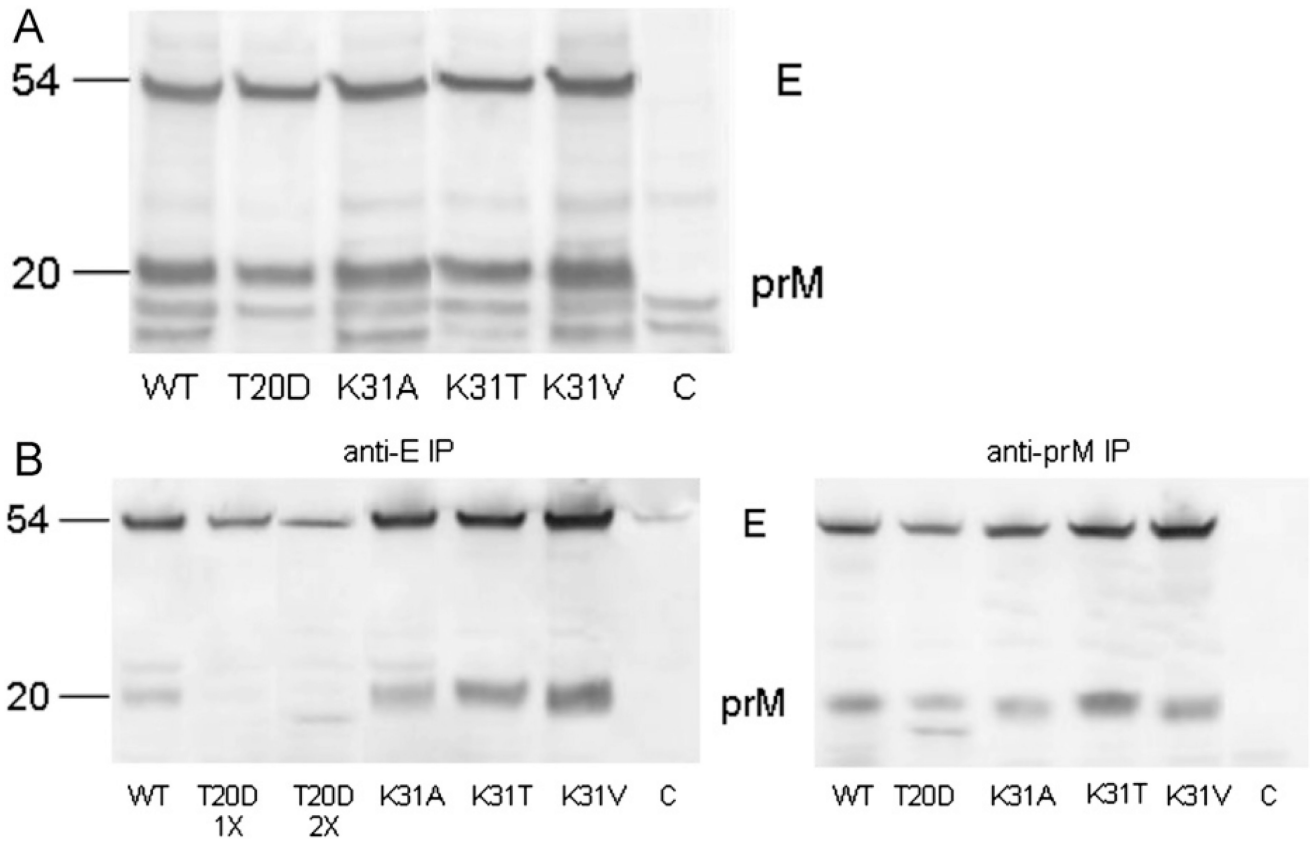

Fig. 2.

Immunoprecipitation of prM and E proteins in COS-1 cells transfected with mutant VLP. COS-1 cells were transfected with WT and mutant pVAXWN plasmids. At 2 days post-transfection, cells were lysed. Whole cell lysates (A) and lysates immunoprecipitated with an anti-E mMAb (3.91D) or an anti-prM hMAb (8G8) (B) were separated by SDS-PAGE on a reduced 4–12% Bis–Tris gel and transferred to nitrocellulose membranes. Proteins bands were detected using anti-E mMAb (3.67G) and anti-prM rabbit polyclonal sera. Non-transfected COS-1 cell lysate was used as a control (C).

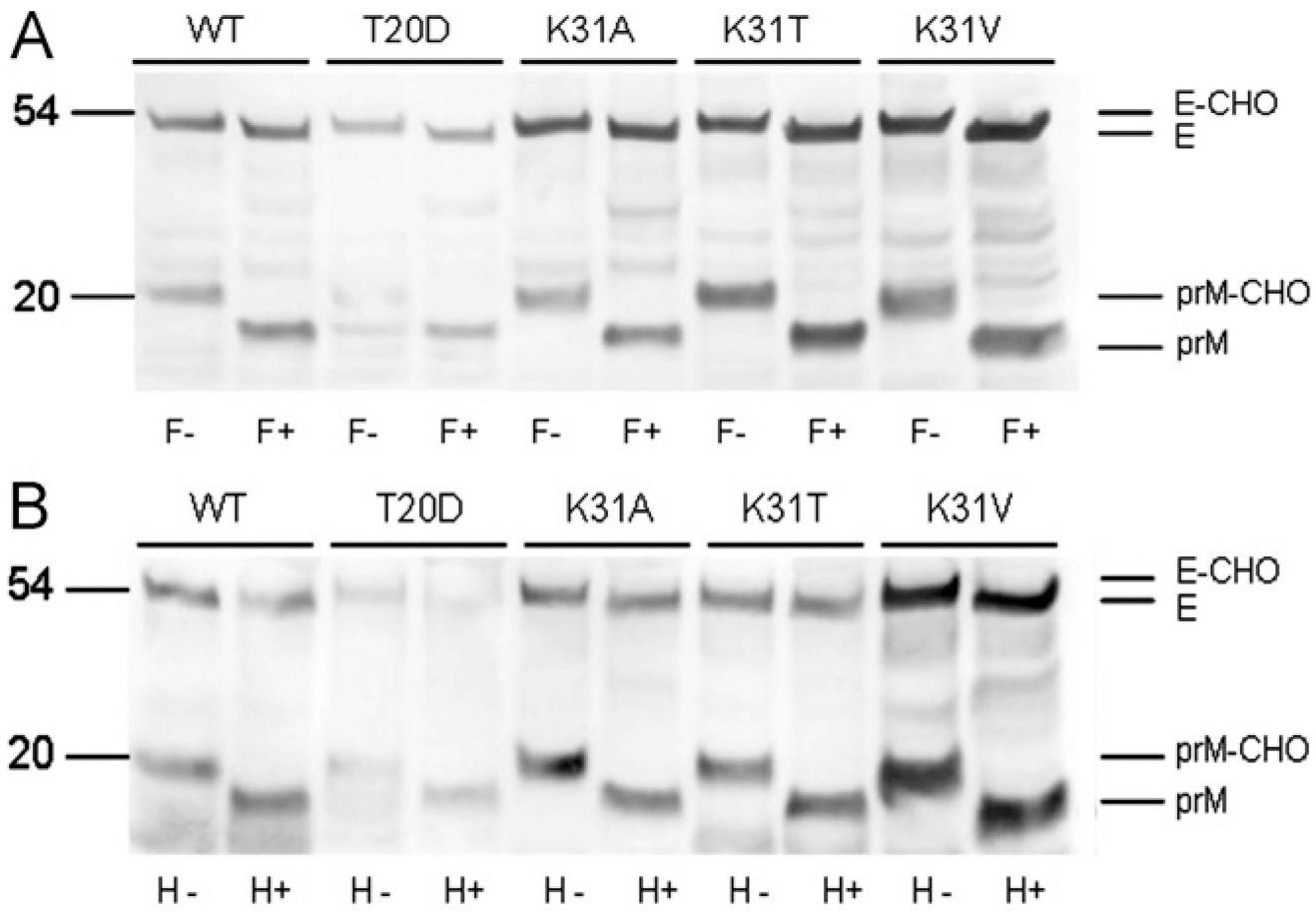

Fig. 3.

Analysis of glycosylation of prM and E proteins in COS-1 cells transfected with mutant pVAXWN plasmids. COS-1 cells were transfected with WT and mutant pVAXWN plasmids. At 48 h post-transfection, cells were lysed. Lysates were immunoprecipitated with an anti-prM hMAb (8G8). Immunoprecipitated proteins were digested with (A) PNGaseF (F+) or without PNGaseF (F−), and with (B) EndoH (H+) or without EndoH (H−). Proteins were separated by SDS-PAGE on a reduced 4–12% Bis–Tris gel and transferred to nitrocellulose membranes. Protein bands were detected using anti-E mMAb, 3.67G, and anti-prM rabbit polyclonal sera.

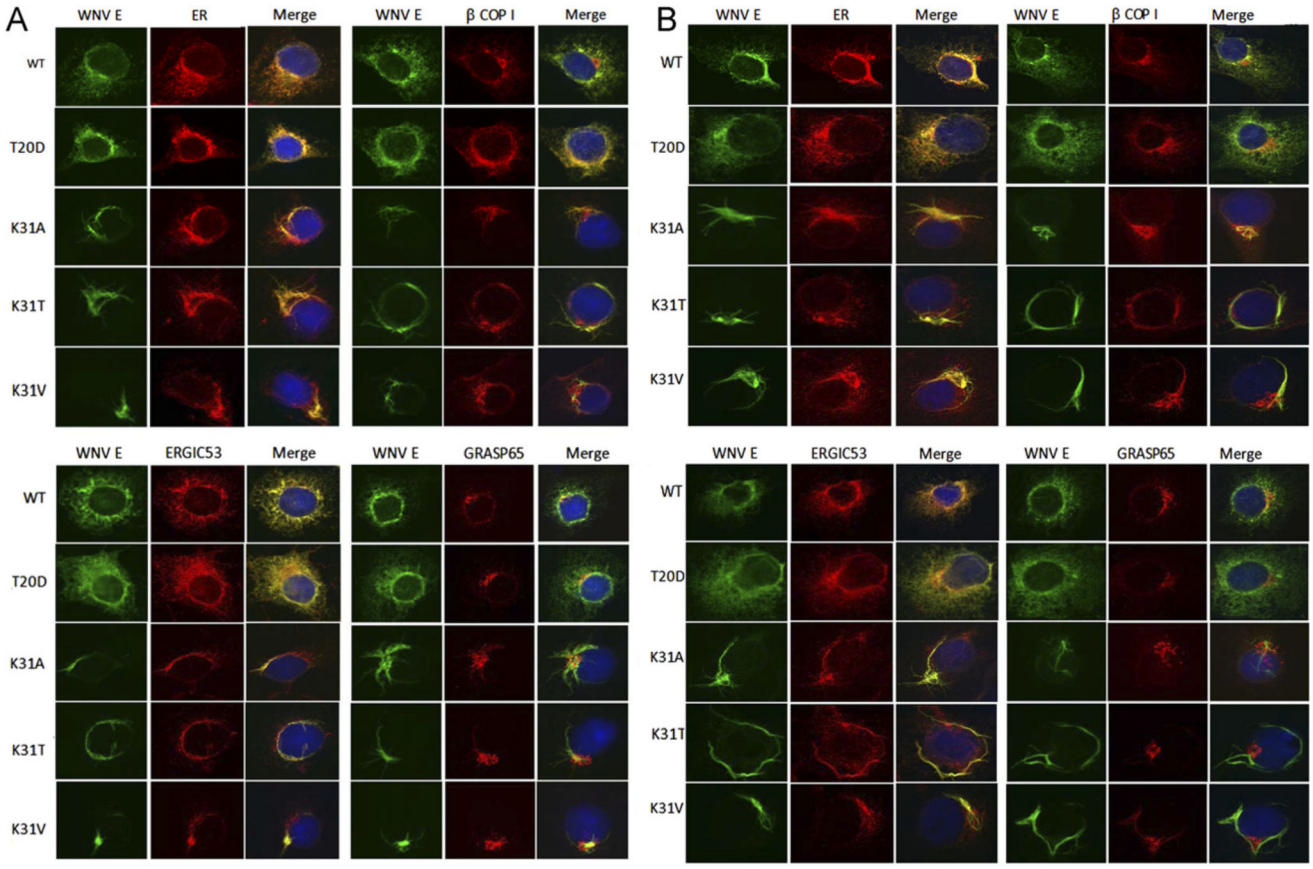

Fig. 4.

Intracellular localization of expressed E proteins of COS-1 cells transfected with prM mutant pVAXWN plasmids. Transfected COS-1 cells expressing pVAXWN WT and prM mutant plasmids were fixed 12 (A) and 24 (B) hours post-transfection and stained with antibodies against WNV E protein (3.91D) and calreticulin, an ER marker, ER–Golgi intermediary complexes βCOP1 and ERGIC53 or GRASP65, a Golgi marker. Co-localization of the E protein with these marker proteins are depicted in the merged image. Nuclei of cells were stained with DAPI and shown in the merged image.

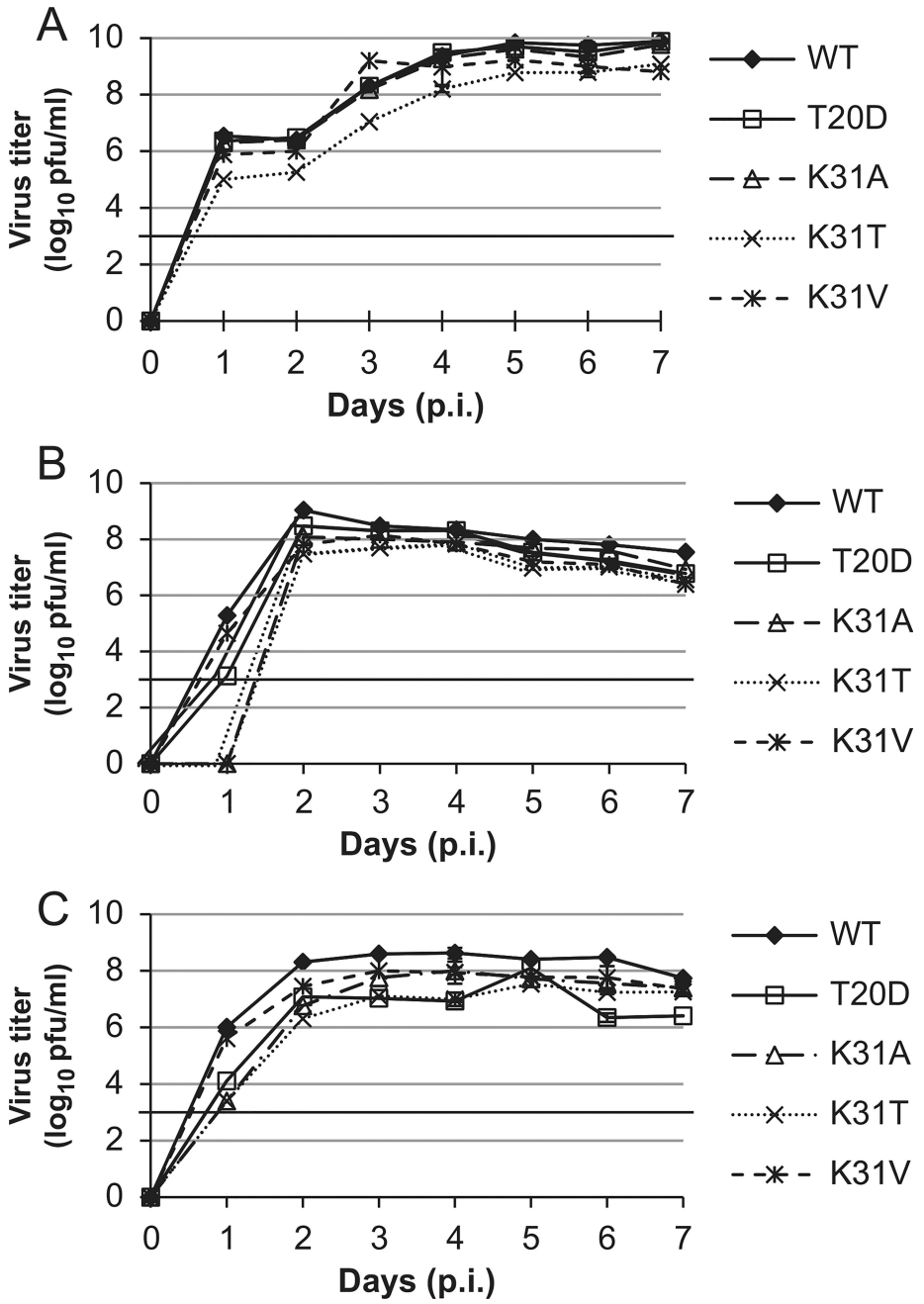

Fig. 5.

Virus growth kinetics in C636, Vero, and COS-1cells. C636 (A), Vero (B) or COS-1 (C) cells were infected at a MOI of 0.1 and virus titers were measured by plaque assay every day for 7 days. Bold line indicates assay limit of detection. Standard error bars are shown for days 4 and 6. The data shown are from two independent experiments.

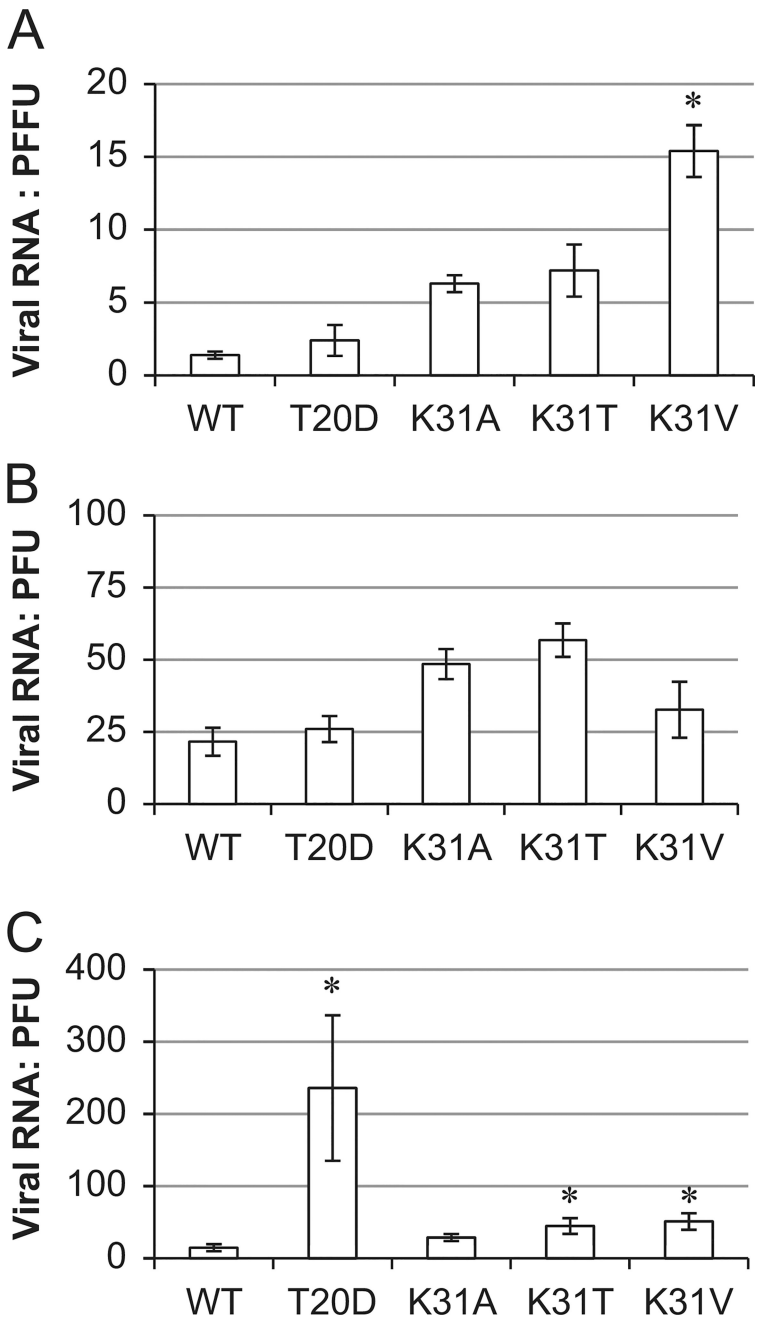

Fig. 6.

Viral RNA:PFU Ratio of prM mutants. Virus was grown in C636 (A), Vero (B), or COS-1 (C) cells and virus supernatant was harvested on days of peak virus titer. RNA was extracted and RNA copies/ml was determined by qRT-PCR. Virus titer was determined by plaque assay. The number of RNA copies/ml was divided by the virus titer to obtain the ratio of RNA copies/ml to PFU/ml. Asterisks indicate statistically significant differences compared to WT virus using Dunnett's method of multiple comparisons with an overall type I error of 0.05. The data shown are from three independent tests. Plaque assays to determine virus titer

were performed in duplicate, while qRT-PCR experiments were performed in triplicate for each independent test.

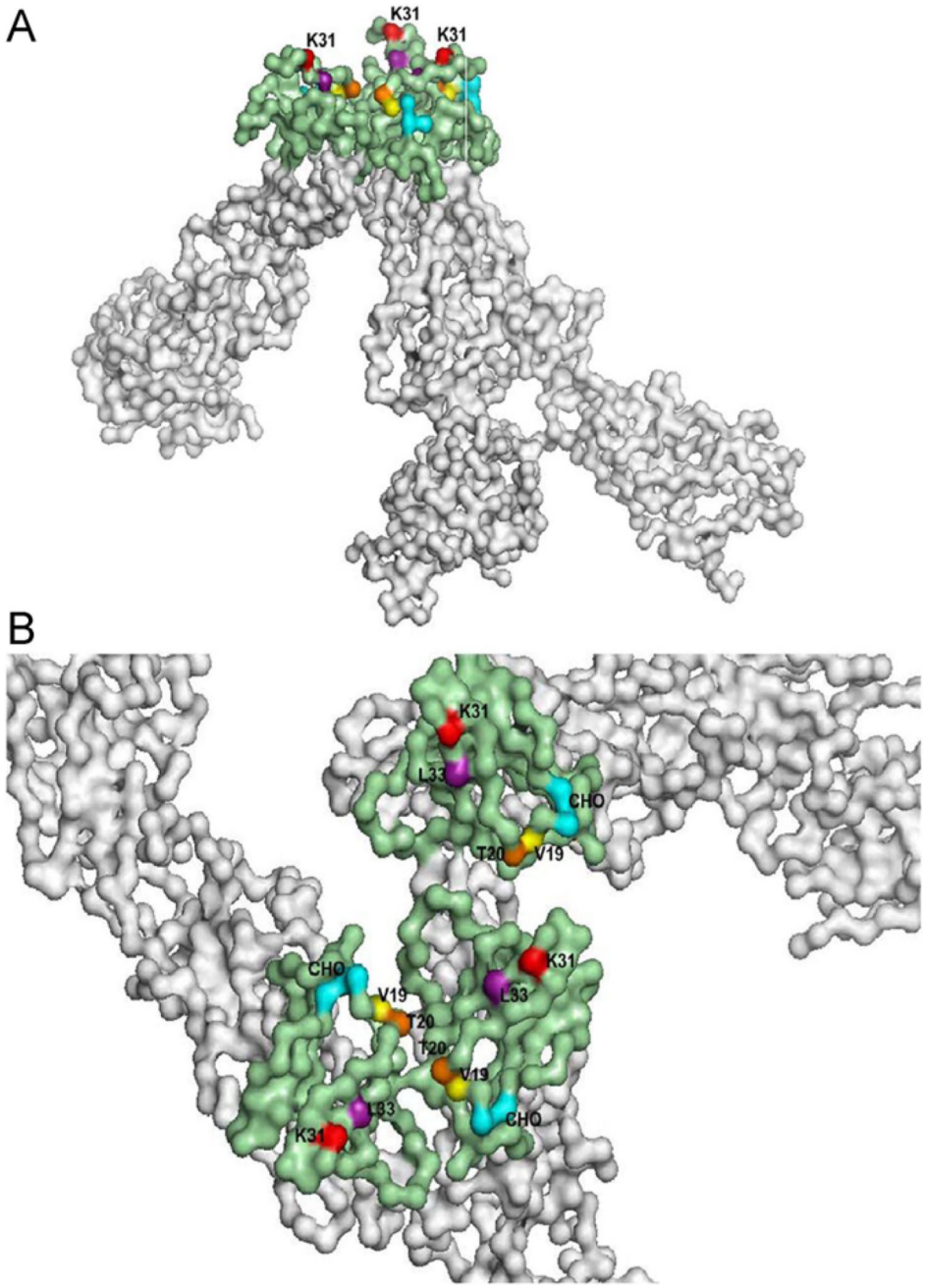

Fig. 7.

DEN2 prM-E trimer spike at neutral pH (PDB ID: 3C6D): (A) side view of the viral surface of the DEN2 prM-E trimer spike and (B) top view toward the viral surface. The E protein is shown in white, while the prM protein is shown in green. V19 is highlighted in yellow, T20 is highlighted in orange, K31 is highlighted in red, L33 is highlighted in purple and the glycosylation site (labeled CHO) is highlighted in cyan.

Table 1

Average plaque sizes of WT and prM mutants viruses.

Cells[a]	Virus plaque size (mm)[b]				
	WT	**T20D**	**K31A**	**K31T**	**K31V**
C636	5.75 ± 1.0	5.35 ± 1.2	3.5 ± 0.9*[c]	2.75 ± 0.7*	4.4 ± 1.2*
Vero	5.6 ± 1.6	5.2 ± 1.2	3.1 ± 0.8*	3.0 ± 1.1*	4.15 ± 1.0*
COS-1	5.85 ± 1.3	5.9 ± 1.0	4.4 ± 1.2*	2.65 ± 0.7*	5.2 ± 1.4

[a] Virus was grown in three different cell types prior to plaque assay in Vero cells.

[b] Average plaque sizes (mean diameters ± standard deviations) were estimated by counting 20 representative plaques.

[c] Significant difference in plaque size compared to WT virus calculated by Dunnett's method of multiple comparisons with an overall type I error of 0.05.

Table 2

Effect of hMAb binding to WNV IC mutant viruses with amino acid substitutions in pr.

pr AA substitution in WNV-IC[a]	Fold change in human Ab titer with pr mutants[b]		
	8G8	5G12	Human sera[c]
WT prM	1.0	1.0	1.0
V19A	2.5	1.7	2.0
V19N	1.5	1.0	1.5
V19T	2.0	1.7	1.5
T20A	3.0	2.0	2.0
T20D	**0.1**	1.7	1.0
T20Q	1.5	1.3	1.0
T24A	1.3	1.5	1.3
K31A	**5.0**	2.7	1.2
K31T	2.7	2.0	2.0
K31V	**4.0**	2.0	2.0
L33A	2.0	2.0	1.3
L33K	2.0	2.0	1.3
L33Q	2.0	1.5	1.3

[a] Amino acid substitution at specific residue in the pr portion. Mutants in bold were previously determined to have a significant effect on VLP-hMAb reactivity.

[b] Four fold reduction or more (bold) in MAb endpoint titer of mutant viruses compared to WT was considered significant.

[c] Human sera positive for anti-flavivirus antibody was used as control in ELISA to verify normalized viral protein concentrations.